Comparison of the accuracy of the calibration model on the double and single integrating sphere systems

A. Singh*[a,b], A. Karsten[a]
[a]Biophotonics Group, National Laser Centre, Council for Scientific and Industrial Research, P. O. Box 395, Pretoria, 0001, South Africa; [b]Laser Research Institute, Department of Physics, University of Stellenbosch, Private bag X1, Matieland, 7602, South Africa

ABSTRACT

The accuracy of the calibration model for the single and double integrating sphere systems are compared for a white light system. A calibration model is created from a matrix of samples with known absorption and reduced scattering coefficients. In this instance the samples are made using different concentrations of intralipid and black ink. The total and diffuse transmittance and reflectance is measured on both setups and the accuracy of each model compared by evaluating the prediction errors of the calibration model for the different systems. Current results indicate that the single integrating sphere setup is more accurate than the double system method. This is based on the low prediction errors of the model for the single sphere system for a He-Ne laser as well as a white light source. The model still needs to be refined for more absorption factors. Tests on the prediction accuracies were then determined by extracting the optical properties of solid resin based phantoms for each system. When these properties of the phantoms were used as input to the modeling software excellent agreement between measured and simulated data was found for the single sphere systems.

Keywords: integrating sphere, light tissue interaction, calibration model

1. INTRODUCTION

Optical methods have been applied to many fields from metallurgy to security but the great strides it has made for biomedical applications in therapeutics and diagnostics requires a better understanding of the interaction of light with tissue. This understanding is based on knowing optical properties such as the absorption and scattering coefficients which affect the fluence distribution in the tissue and the safe optimum dose for treatment or diagnosis. This then requires that the optical properties be accurately known. The important properties are the absorption, scattering, reduced scattering coefficients, anisotropy factor and refractive index (μ_a , μ_s , μ'_s , g and n). The best known and simplest method by which the former four optical properties of tissue *in vitro* can be determined is using the Integrating Sphere (IS).

Measurement of tissue optical properties using either the single or double IS setup is well documented in literature[1,2]. However the variance in the actual values in the literature is huge. This could be attributed to the state of the *in vitro* tissue or the method used to determine such properties[3,4]. There is also not an extensive database available for all the tissue types at the required wavelengths for treatment and diagnostics. The need for this study was thus two fold. One of the goals is to build up an extensive database of the optical properties of different tissue types for the important wavelengths. Due to the different constituents of tissue, the properties will change depending on the wavelength used.

Our particular interest is in skin, the largest organ in the body, because most minimally invasive optical techniques need to penetrate through skin. Furthermore skin cancer is an increasing problem in South Africa and is further complicated by a large variance in skin types or skin tone. To the best of our knowledge the optical properties of skin tone has not been investigated extensively[5]. Thus it was imperative to find a simple method by which to characterize the different skin types which is our second goal. However the determination of optical properties is an inverse problem and thus the accuracy of such properties is highly dependant on the accuracy of the calibration model. Hence the aim of this work was to determine the accuracy of the calibration model created for white light (WL). The existence of both the double and single IS systems allowed us to compare the accuracy for both systems.

*asingh1@csir.co.za; phone 2712 841 4650; fax 2712 841 3152.

International Symposium on Photoelectronic Detection and Imaging 2011: Laser Sensing and Imaging; and Biological and Medical Applications of Photonics Sensing and Imaging, edited by Farzin Amzajerdian, Weibiao Chen, Chunqing Gao, Tianyu Xie, Proc. of SPIE Vol. 8192, 81924U · © 2011 SPIE · CCC code: 0277-786X/11/$18 · doi: 10.1117/12.899879

This paper will review the two IS setups, the calibration model created for WL at 632.8 nm, the verification of the calibration model with solid resin based phantom measurements and light propagation modeling using Advanced Systems Analysis Program (ASAP) (Breault Research Organization, Inc.).

2. METHODOLOGY

2.1 Setup and Measurements

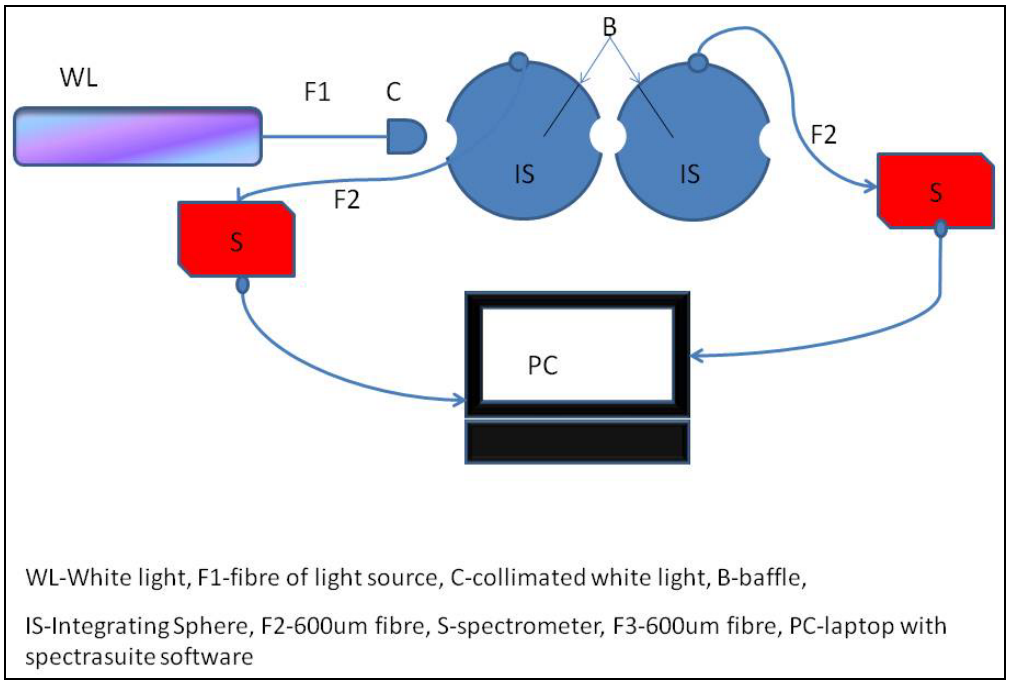

Figure 1 Illustration of the Double Integrating Sphere setup

The double IS setup is shown in figure 1. A supercontiniuum white light source (Koheras) is incident on the entrance port of the 2 spheres (6 inch diameter (Labsphere)). The spheres are aligned such that the baffle on each sphere is between the sample and the detector. The signal on each sphere is detected by a (600 μm core diam) fibre coupled spectrometer (Ocean Optics USB4000) connected to a laptop. Diffuse and total transmittance as well as diffuse reflectance measurements are taken in triplicate for each sample. This data is extracted for different wavelengths and recorded as a function of μ_a and μ'_s. Different order polynomials are used to fit the measured data to the simulated values and determining the prediction errors. To obtain the optical properties, the measured data is fitted to the calibration model by applying the multiple polynomial regression method and the Newton-Raphson algorithm[6,7].

The single IS setup looks very similar to figure 1 with the exception that the sphere has an 8 inch diameter. The setup is aligned such that the double and single IS setups are on the same axis. Data acquisition and analysis remains the same.

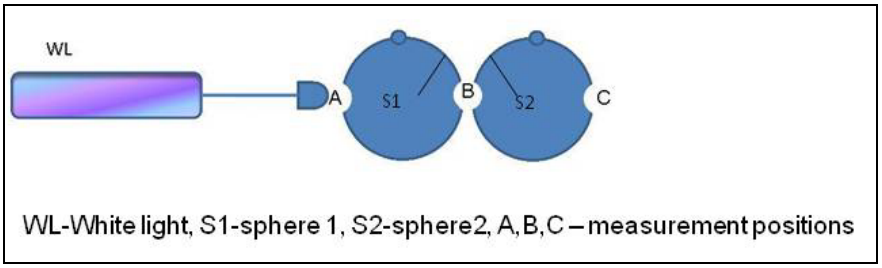

Figure 2: Configuration for measurement

Figure 2 shows the configuration for the measurements. Dark measurements are taken with no sample at B and no reference at C. A measurement is taken on both spheres (T_B , R_B). A reference standard (95-98% reflective) is placed at C and measurements taken on sphere 2(T_R). Another reference is taken by placing the reference standard at B, measure on sphere 1 (R_R). For diffuse transmittance and reflectance the sample is placed at B and a measurement taken on each sphere (T_D R_D) respectively. To measure the total transmittance the sample is placed at B and the reference standard at C and a measurement taken on sphere 2 (T_T).

For the single sphere assume the same setup as figure 2 excluding sphere 2 and point C. A measurement is taken for no sample or reference standard (S_B). A reference measurement is taken by placing the reference standard at B (S_R). For diffuse transmittance sample is placed at A (T_{DS}). For total transmittance sample at A and reference standard at B (T_{TS}) and for diffuse reflectance, the sample is placed at B (R_{DS}).

2.2 Calibration model

Intralipid (IL) and black ink are used for the calibration model. It is assumed that the IL only has scattering properties and does not absorb light in the visible part of the spectrum. The ink is assumed to be totally absorbing. Different concentrations of 3 ml IL (Sigma Aldrich, lot # 028K0740) samples were prepared using 11.04 cm^{-1} ×IL conc[8]**.** Ink solutions were made up with different amounts of pure black ink in 50 ml water. The Beer Lambert law $I = I_o e^{-\mu_t \cdot d}$ was used to calculate μ_a. The intralipid and ink solutions were mixed in equal proportion to create a phantom with well defined optical properties. We assume that the μ_a and μ'_s in the phantom is half that in the original samples based on the assumptions that the intralipid is non-absorbing and the ink solution non-scattering. The elements of the matrix of the model were in the range $0.55 \le \mu_a \le 3.28 cm^{-1}$ and $0.552 \le \mu'_s \le 110.4 cm^{-1}$ at 632.8nm. The range of the calibration model should ideally cover the range of the expected optical properties of tissue. Samples were poured into a 1.5 mm cuvette shown in figure 3 to be measured.

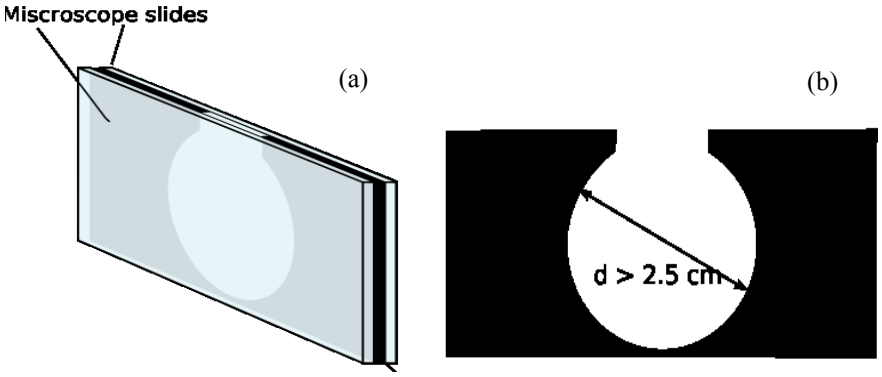

Figure 3: Cuvette and spacer used

2.3 Verification of Model

Solid resin based phantoms were made up and measured on the double and single IS setups for the white light as well as on the single IS setup using a He-Ne calibration model. The optical properties for the phantom was extracted for the different setups and used in the ASAP software to determine the transmission through and reflectance of the sample based on the optical properties. These were then compared against the measured total transmittance and diffuse reflectance for each sample. The ASAP program used has been verified to be a good working model for light-tissue interaction[9].

3. RESULTS AND DISCUSSION

3.1 Calibration model

The results in Figure 4,5,6 and Table 1 showed a very good fit for the data using the third order polynomials for the single sphere model for the He-Ne used in previous investigations [3,5,7,9] and the while light (WL-S). Figures 4,5 represent the mean errors of prediction (MEP) when trying to predict the elements found on any position (including boundary elements) in the matrix of the model. This allows us to use, with confidence, the third order predictions for μ_a and μ'_s of the single sphere model for He-Ne and WL-S. Currently the data for the Double sphere model (WL-D) indicate very high prediction errors. It was seen that this is due to inaccuracies in the measurement data for some of the solutions. Many of these points have been excluded but it significantly reduces the range of values which can be used for the predictions. The reason for the inaccuracies may be due to the positioning of the sample and the method of taking a reference. More data points will be added to extend the model and then test the prediction accuracies. This work is currently underway. The model for WL-S also needs to be expanded for more ink solutions so that a more even distribution as seen by the He-Ne model is in place. A finer increment model should give more accurate results.

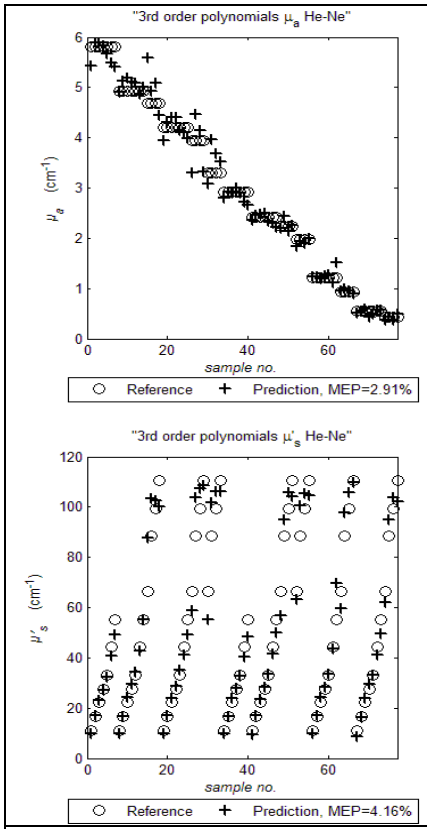

Figure 4: Prediction fit for He-Ne model

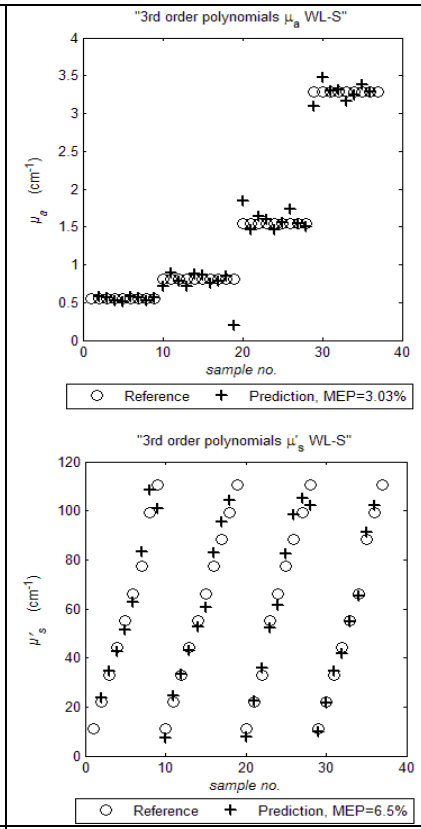

Figure 5: Prediction fit for WL-S model

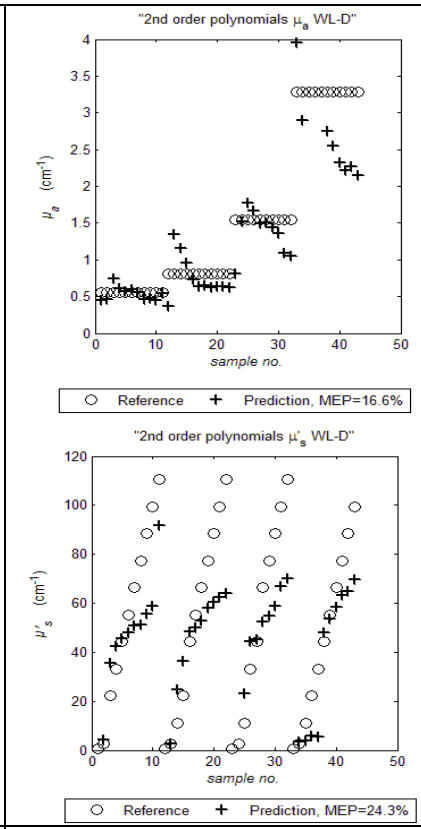

Figure 6: Prediction fit for WL-D model

Table 1: Comparison of % errors in predicting μ_a and μ'_s for the different models

	μ_a 2	μ_a 3	μ_a 4	μ'_s 2	μ'_s 3	μ'_s 4
He-Ne inner	4.95	2.87	2.2	7.18	4.30	2.40
He-Ne entire	16.80	2.91	7.29	>100*	4.16	>100*
WL-S-inner	2.32	2.37	14.19	6.84	4.11	12.06
WL-S-entire	22.80	3.03	19.60	20.30	6.50	16.25
WL-D-inner	6.90	22.70	37.35	14.00	>100	>100
WL-D-entire	16.60	24.90	44.97	24.30	>100	>100

*good fits are evident but 1 or 2 outliers in the data cause the prediction errors to become very large

The data shown in table 1 indicates why the third order predictions have been chosen for extracting the optical properties. They give the lowest errors irrespective of whether the properties of the samples lie within the matrix of the model or the boundaries of the model. For WL-D the 'best' choice would be the second order predictions, however these errors are too high to use the model with confidence.

3.2 Verification of Calibration model

Having shown that the single sphere models gave low prediction errors we needed another way to test the accuracy of our predictions. Having worked with the He-Ne model previously with some good comparison to literature [7] we thought it best to test this against the ASAP model[9,10]. To do this a set of solid resin phantoms were prepared. The diffuse reflectance (R) and total transmittance (T) were measured and the optical properties extracted. These properties were then used in the program to calculate the transmission and reflectance of the phantom.

Table 2: Verification of He-Ne model with ASAP model

Sample	IS T	ASAP T	IS R	ASAP R
A1	0.33	0.34	0.52	0.50
A3	0.25	0.25	0.41	0.38
B1	0.39	0.41	0.38	0.33
B3	0.39	0.41	0.35	0.30

As shown by the results in table 2, the agreement between the ASAP model and actual IS measurements was great. The combined low error predictions of the He-Ne model as well as the agreement with ASAP meant the He-Ne model could be used as a benchmark for WL-S and WL-D. The next step was to compare the actual predicted values of μ_a and μ'_s for the different IS models. Phantoms were again prepared and measured.

Table 3: Comparison of the predicted μ_a and μ'_s for the solid phantoms using the different models

Sample	μ_a 3 He-Ne	μ_a 3 WL-S	μ_a 2 WL-D	μ'_s 3 He-Ne	μ'_s 3 WL-S	μ'_s 2 WL-D
A1	0.041	0.05	0.005	13.27	14.50	1.23
A2	0.05	0.07	0.004	11.10	11.65	0.93
A3	0.11	0.17	0.01	10.64	11.90	1.42
B1	0.07	0.08	0.001	5.47	6.84	1.31
B2	0.07	0.08	0.01	5.35	7.01	1.38
B3	0.08	0.12	0.01	5.09	6.11	1.44

Most of the results shown in Table 3 indicate good agreement between the two single sphere models. The disagreements that arise may be a combination of the inherent inaccuracies of each model and the inaccuracies in real time measurements. Data for WL-D is shown but as expected from the prediction results there is at least a factor of 10 difference with the data for WL-S.

The last test in this series of experiments was to compare the data of WL-S to ASAP. Results shown in table 4 showed consistent good agreement between measured and simulated data. This in combination with the good agreement between He-Ne and WL-S has for our current data series validated WL-S as a good working model in comparison to WL-D. It should be noted that the μ_a values of the phantoms measured fall outside the boundaries of our models but was successfully predicted by both single sphere models. This is an excellent result. This good working model for WL-S at 632.8nm can serve as a comparison for the calibration of the other wavelengths. This will then mean that a single measurement on the white light system will yield optical properties at all the desired wavelengths.

Table 4: Comparison of ASAP model data for R and T to IS measurements using data from table 2 for WL-S

Sample	IS T	ASAP T	IS R	ASAP R
A1	0.36	0.34	0.37	0.41
A2	0.39	0.38	0.26	0.21
A3	0.31	0.29	0.35	0.33
B1	0.49	0.51	0.30	0.32
B2	0.51	0.50	0.17	0.17
B3	0.35	0.35	0.24	0.18

4. CONCLUSION

It has been shown that the WL-S model is a good working model for the prediction of μ_a and μ'_s at 632.8 nm for the current setup with the white light source. Much more work still needs to be done on WL-D to get a good working model before a conclusion can be made as to the accuracy of the single sphere system to the double sphere system. The white light models do need to be extended over a larger range for μ_a to get a more even stepsize between μ_a for better accuracy of the model.

Acknowledgements

The authors would like to acknowledge Bafana Moya for the setting up of and measurements done on the IS system. The National Research Foundation (NRF) as well Biophotonics group, National Laser Centre, CSIR for financial support.

REFERENCES

[1] Bashkatov N., Genina E.A., Kochubey V.I and Tuchin V.V, "Optical properties of human skin, subcutaneous and mucous tissues in the wavelength range from 400 to 2000 nm," J. Phys. D: Appl. Phys. 38, 2543-2555 (2005).

[2] Pickering J.W., Prahl S.A, van Wieringen N., Beek J.F, Sterenborg H.J.C.M. and van Gemert M.J.C, ''Double integrating-sphere system for measuring the optical properties of tissue,'' Appl. Opt. 32, 399–410 (1993).

[3] Singh A., Karsten A.E., Smith RM and Van Niekerk G., "Determination of the optical properties of rat tissue. European Cells and Materials," Vol. 19(Suppl. 1), pp 14 (2010).

[4] Nilsson A.M., Sturesson K.C, Liu D.L. and Andersson-Engels S., "Changes in spectral shape of tissue optical properties in conjuction with laser-induced thermotherapy," Appl. Opt. 37 1256–6 (1998).

[5] Karsten A.E., "Effect of Wavelength, Epidermal Thickness and Skin Type on the Required Dose for Photodynamic Therapy," International Conference of the World Association of Laser Therapy, South Africa, 137-143 (2008).
[6] Dam J. S., Dalgaard T., Fabricius P. E. and Andersson-Engels S., "Multiple polynomial regression method for determination of biomedical optical properties from integrating sphere measurements", Appl. Opt 39, 1202-1209 (2000).
[7] Singh A., Karsten A.E. and Dam J.S., "Robustness and Accuracy of the Calibration Model for the Determination of the Optical Properties of Chicken Skin," International Conference of the World Association of Laser Therapy, South Africa, 165-169 (2008).
[8] Michielsen K., De Raedt H., Przeslawski J. and Garcia N., "Computer simulation of time-resolved optical imaging of objects hidden in turbid media," Physics Reports 304 pp 89-144(1998).
[9] Karsten A.E, Singh A. and Braun M.W.H, " Experimental verification and validation of a computer model for light–tissue interaction," (2011) (Accepted for publication in Lasers in Medical Science)
[10] Karsten A.E, Singh A., "Sensitivity of light interaction computer model to the absorption properties of skin," ISPDI 2011 Symposium, China (2011).